

An Investigation of Two Novel Pyridazine Derivatives as Corrosion Inhibitor for C38 Steel in 1.0 M HCl

A. Ghazoui¹, N. Bencaht¹, S. S. Al-Deyab², A. Zarrouk^{1,*}, B. Hammouti¹, M. Ramdani¹, M. Guenbour³

¹ LCAE-URAC18, Faculté des Sciences, Université Mohammed 1^{er}, Oujda, Morocco

² Petrochemical Research Chair, Chemistry Department, College of Science, King Saud University, P.O. Box 2455, Riyadh 11451, Saudi Arabia.

³ Laboratoire d'Electrochimie, Corrosion et Environnement, Faculté des Sciences, Rabat, Morocco.

* E-mail: azarrouk@gmail.com

Received: 10 October 2012 / Accepted: 7 January 2013 / Published: 1 February 2013

Corrosion inhibition of two pyridazine derivatives, namely ethyl (6-oxo-3-phenylpyridazin-1(6H)-yl)acetate (GP2) and ethyl (3-phenyl-6-thioxopyridazin-1(6H)-yl)acetate (GP3) on C38 steel was investigated by gravimetric measurements, polarisation and electrochemical impedance spectroscopy (EIS). Gravimetric measurements indicate that the inhibitor GP3 is more effective than GP2 for protection against C38 steel corrosion in 1.0 M HCl medium. The protective power of these products increases with increasing concentration but decreases with rise temperatures. The effectiveness of inhibition reached 91.83% and 83.90% for GP3 and GP2 respectively at 10⁻³M. Moreover, Potentiodynamic polarisation studies revealed that the inhibitors act as mixed inhibitors. The inhibition occurs through adsorption of the pyridazine compounds on the metal surface without modifying the mechanism of corrosion process. EIS shows that increasing the concentration of the inhibitors leads to an increase of the charge transfer resistance and reducing the double layer capacitance. Effect of temperature was studied between 308 and 343 K and determination of activation parameters and adsorption is also discussed.

Keywords: Pyridazine derivatives, Steel, Corrosion inhibition, Polarization curves, EIS.

1. INTRODUCTION

Acid solutions are extensively used in a variety of industrial processes such as oil well acidification, acid pickling and acidic cleaning [1], which generally lead to serious metallic corrosion. Organic compounds, corrosion inhibitors, are widely used in industry to prevent corrosion in acidic environments [2–6]. The addition of inhibitors is one of the most practical methods of corrosion protection. Among them, heterocyclic compounds containing nitrogen, phosphorus, sulphur, oxygen

and aromatic rings are the most effective and efficient inhibitors for the metals in acidic medium due to their special molecular structure [7–17]. Several studies have shown that N-heterocyclic compounds such as pyridazines [18–28], are well qualified to protect steel against corrosion.

Nowadays the search for new and efficient corrosion inhibitors has become a necessity to secure metallic materials against corrosion. The effectiveness of organic compounds containing sulphur as corrosion inhibitors for steels in sulphuric acid is well developed [19–35]. The adsorption of inhibitors takes place through heteroatoms such as nitrogen, oxygen, phosphorus and sulphur, triple bonds or aromatic rings. The inhibition efficiency should increase in the order $O < N < S < P$ [36].

The introduction of sulphur atom in heterocyclic compounds containing nitrogen, has proved very good for inhibitors for the corrosion of metals in acidic solutions [37,38]. Their inhibitive power is related to the various active centers of adsorption as cyclic rings or heteroatoms. Past studies have proved the pyridazine derivatives containing sulphur atom offer good inhibitory effect of the corrosion of steel in acidic media [28]. The choice of pyridazine compounds is based on their much known pharmaceutical application in inhibiting aldose reductase and exhibiting antioxidant properties [39, 40] and the presence of two nitrogen atoms in pyridazine ring with various substituents.

In the present paper, two newly tested pyridazine derivatives as corrosion inhibitors for C38 steel in 1.0 M HCl using gravimetric measurement, potentiodynamic polarization methods and electrochemical impedance spectroscopy at various concentrations ($10^{-6}\text{M} - 10^{-3}\text{M}$) of GP2 and GP3. A comparative inhibition study was investigated and studied. Effect of temperature is studied between 308 and 343 K and determination of activation and adsorption parameters. The chemical structures of the studied pyridazine derivatives are given in Fig.1.

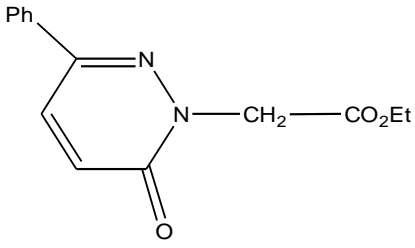
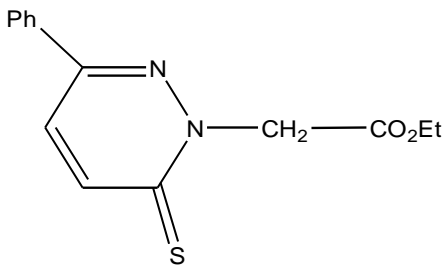
Pyridazine name	Chemical Structure	Abbreviation
ethyl (6-oxo-3-phenylpyridazin-1(6H)-yl)acetate		GP2
ethyl (3-phenyl-6-thioxopyridazin-1(6H)-yl)acetate		GP3

Figure 1. The chemical structure of the studied pyridazine compounds.

2. EXPERIMENTAL PART

2.1. Materials, reagents and Synthesis

In order to obtain reliable and reproducible results, the samples are prepared Mild steel before each test by polishing with abrasive paper of grain size finer "TINGIS" (grade 100-400-800-600-1200), followed by rinsing with bidistilled water, and finally the sample is dried under a stream of air.

The chemical composition in weight of steel samples used in this study is as follows (0.09% P, 0.38% Si, 0.01% Al, 0.05% Mn, 0.21% C, 0.05% S and the balance iron). The molar solution of hydrochloric acid (1.0 M HCl) is obtained by dilution of concentrated acid density $d = 1.18$ and 35.4% by weight with distilled water.

2.2. Measurements

2.2.1. Weight loss measurements

The steel sheets of $1.6 \times 1.6 \times 0.07$ cm dimensions were abraded with different grades of emery papers, washed with distilled water, degreased with acetone, dried and kept in a desiccator. After weighing accurately by a digital balance with high sensitivity the specimens were immersed in solution containing 1.0 M HCl solution with and without various concentrations of the investigated inhibitors. At the end of the tests, the specimens were taken out, washed carefully in ethanol under ultrasound until the corrosion products on the surface of C38 steel specimens were removed thoroughly, and then dried, weighed accurately. Duplicate experiments were performed in each case and the mean value of the weight loss is reported. Weight loss allowed calculation of the mean corrosion rate in $\text{mg cm}^{-2} \text{h}^{-1}$.

2.2.2. Electrochemical measurements

The electrochemical measurements were carried out using Volta lab (Tacussel- Radiometer PGZ 301) potentiostat and controlled by Tacussel corrosion analysis software model (Voltmaster 4) at under static condition. The corrosion cell used had three electrodes. The reference electrode was a saturated calomel electrode (SCE). A platinum electrode was used as auxiliary electrode of surface area of 1 cm^2 . The working electrode was C38 steel. All potentials given in this study were referred to this reference electrode. The working electrode was immersed in test solution for 30 minutes to establish steady state open circuit potential (E_{ocp}). After measuring the E_{ocp} , the electrochemical measurements were performed. All electrochemical tests have been performed in aerated solutions at 308 K. The polarization curves were obtained in the potential range from -800 to 200 mV_{SCE} with 1 mV s^{-1} scan rate. The EIS experiments were conducted in the frequency range with high limit of 100 kHz and different low limit 0.1 Hz at open circuit potential, with 10 points per decade, at the rest potential, after 30 min of acid immersion, by applying 10 mV ac voltage peak-to-peak. Nyquist plots were made from these experiments. The best semicircle can be fit through the data points in the Nyquist plot using a non-linear least square fit so as to give the intersections with the x -axis.

3. RESULTS AND DISCUSSION

3.1. Gravimetric measurements

3.1.1. Effect of concentration

The mass loss measurements were conducted for an immersion time of 6 hours at 308 K kept constant, with and without addition of GP2 and GP3 pyridazines at various concentrations under normal ventilation. This measurement method allows to directly assessing the corrosion rate, this value can be calculated by equation (1):

$$W_{corr} = \frac{\Delta m}{St}$$

With $\Delta m = (m_i - m_f)$ mass loss in mg, m_i the initial mass, m_f final mass, t the immersion time (hours) and S the total area of the sample in cm^2 etching solution maintained at constant temperature, W_{corr} the corrosion rate ($\text{mg cm}^{-2} \text{h}^{-1}$).

The determination of the effectiveness inhibitory (protective power of an inhibitor) of these organic compounds using the relation (2):

$$E_w \% = \left(1 - \frac{W_{corr}}{W_{corr}^{\circ}} \right) \times 100$$

Table 1. Gravimetric results of C38 steel in 1.0 M HCl at different concentration of each inhibitor at 6h and 308 K.

Inhibitors	Conc (M)	W_{orr} ($\text{mg}/\text{cm}^2 \text{ h}$)	E_w (%)	θ
Blank	1.0	1.142	-----	-----
GP2	1×10^{-3}	0.183	83.9	0.839
	5×10^{-4}	0.197	82.7	0.827
	1×10^{-4}	0.302	73.5	0.735
	5×10^{-5}	0.384	66.3	0.663
	1×10^{-5}	0.585	48.7	0.487
	1×10^{-6}	0.688	39.6	0.396
GP3	1×10^{-3}	0.093	91.8	0.918
	5×10^{-4}	0.101	91.2	0.912
	1×10^{-4}	0.243	78.7	0.787
	5×10^{-5}	0.336	70.5	0.705
	1×10^{-5}	0.493	56.7	0.567
	1×10^{-6}	0.664	41.8	0.418

Where W_{corr} and W_{corr}° are the corrosion rates of steel in the presence and absence of inhibitors, respectively. The fractional surface coverage θ can be easily determined from the weight loss

measurements by the ratio $E_w (\%)/100$, where $E_w (\%)$ is inhibition efficiency and calculated using relation 2.

We gathered in Table 1, the values of the corrosion rate and inhibition efficiency, which represent the average of three tests for different concentrations of pyridazine compounds tested under the same experimental conditions.

The analysis of the values given in this table clearly shows a net decrease of the corrosion rate of C38 steel in 1.0 M HCl medium in the presence of GP2 and GP3 our pyridazines. In other words, their inhibition efficiency increases with the concentration reaching the maximum value of 91.83% for GP3 and 83.90% for GP2 at 10^{-3} M.

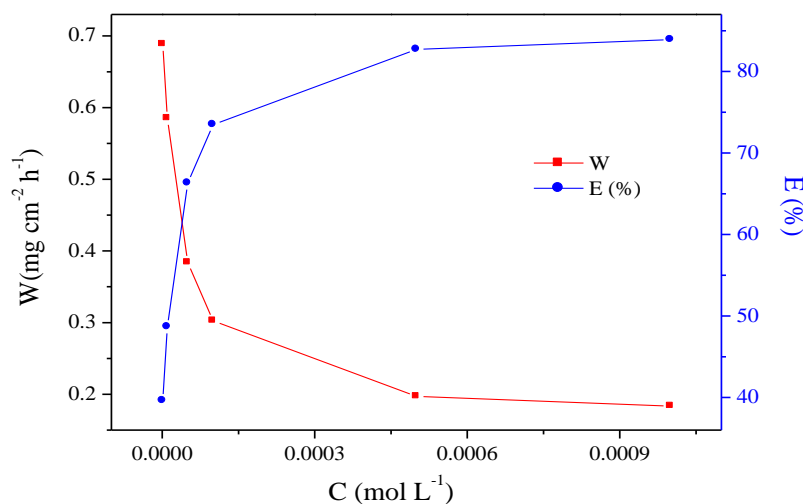


Figure 2. Variation of inhibition efficiency and corrosion rate in 1.0 M HCl on C38 steel surface without and with different concentrations of GP2.

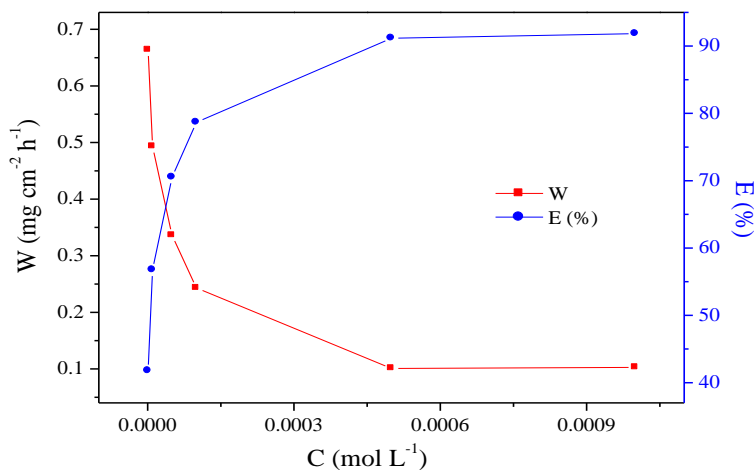


Figure 3. Variation of inhibition efficiency and corrosion rate in 1.0 M HCl on C38 steel surface without and with different concentrations of GP3.

This increased efficiency of inhibition shows that our molecules can be adsorbed onto the surface to cover the active sites of the surface of the electrode. The comparative study of the inhibitory potency of tested pyridazines shows that the inhibition efficiency to GP3 is higher than to GP2 at 10^{-3} M. The high efficiency of inhibitory GP3 can be attributed to the presence of the thiooxo group (C = S) on the pyridazine ring, which gives the possibility of $d\pi-d\pi$ bond formation resulting from overlap of 3d electrons from Fe atom to the 3d vacant orbital to the sulphur atom [41]. Brandt et al. [42] reported that the sulphur atom is the active centre of the aliphatic sulphides in their interaction with the metal surface. The presence of the sulphur atom causes a drastic change in its adsorption mechanism; these results are in good agreement with results obtained by Chetouani et al. [18, 20].

3.1.2. Effect of temperature and thermodynamic activation parameters

Being given that the temperature is one of the factors that may affect the behavior of a material in a corrosive environment, and can also modify the metal-inhibitor interaction, it is essential to study the effect of this factor on the protection rates, as well to determine the mechanism of inhibition, that for calculating the activation energies of the corrosion process.

The study of the influence of temperature on the rate of corrosion inhibition of C38 steel by our inhibitors were performed at temperatures 308, 313, 323, 333 and 343K in the absence and in the presence of inhibitor at 10^{-3} M for 1h immersion. This study to determine the activation energies, enthalpies and entropies of activation of the corrosion process and thus provides information on the mechanism of inhibition. The corresponding data are shown in Table 2.

Table 2. Various corrosion parameters for steel in 1.0 M HCl in absence and presence of optimum concentration of GP2 and GP3 at different temperatures at 1h.

Temp (K)	Inhibitors	W_{corr} ($\text{mg cm}^{-2} \text{h}^{-1}$)	E_w (%)	θ
308	Blank	1.142	-----	-----
	GP2	0.183	83.9	0.839
	GP3	0.093	91.8	0.918
313	Blank	1.580	-----	-----
	GP2	0.313	80.2	0.802
	GP3	0.173	89.0	0.890
323	Blank	3.030	-----	-----
	GP2	0.822	72.9	0.729
	GP3	0.591	80.1	0.805
333	Blank	5.150	-----	-----
	GP2	2.057	60.1	0.601
	GP3	1.651	67.9	0.679
343	Blank	9.000	-----	-----
	GP2	5.054	43.8	0.438
	GP3	4.837	46.2	0.462

The comparative study of Table 2 showed that the corrosion rate increases with increase in temperature in both the stabilized solutions and inhibited, while the efficiency of inhibiting GP2 and GP3 products decreases. A decrease in the efficiency of inhibition with increasing temperature in the presence of our compounds may be due to the weakening of physical adsorption.

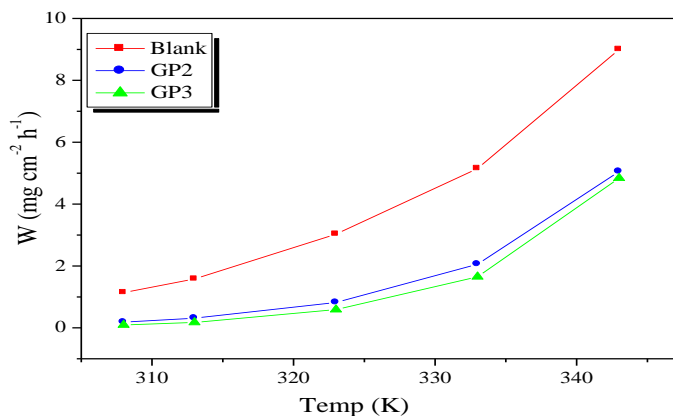


Figure 4. Variation of corrosion rate in 1.0 M HCl on steel surface without and with of optimum concentration of GP2 and GP3 at different temperatures.

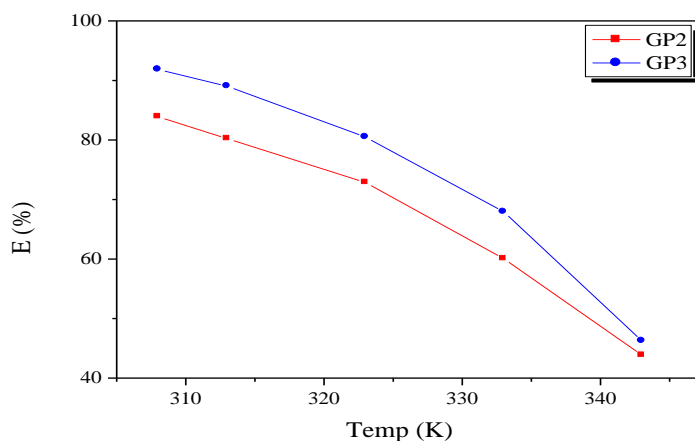


Figure 5. the variation in the inhibition efficiency of GP2 and GP3 obtained measured gravimetrically at different temperatures.

To determine the activation energy, use is made of the Arrhenius equation (3) to account for the effect of temperature (T) on the corrosion rate (W_{corr}), the change in the log the corrosion rate as a function of the reciprocal of the absolute temperature is a linear function of T^{-1} , the corresponding relation (4) provides access to the activation energies:

$$W_{corr} = K \exp\left(-\frac{E_a}{RT}\right) \tag{3}$$

$$\ln W_{corr} = -\frac{E_a}{RT} + \ln A \tag{4}$$

To access the activation thermodynamic characteristics, enthalpy (ΔH_a) and entropy of activation (ΔS_a), we used the Arrhenius equation transition [43]:

$$W_{corr} = \frac{RT}{Nh} \exp\left(\frac{\Delta S_a}{R}\right) \exp\left(-\frac{\Delta H_a}{RT}\right) \tag{5}$$

Where W_{corr} is the corrosion rate, R the gas constant, T the absolute temperature, A the pre-exponential factor, h the Plank's constant and N is Avogrado's number, E_a the activation energy for corrosion process, ΔH_a the enthalpy of activation and ΔS_a the entropy of activation.

The curves of variation of the logarithm of the corrosion rate as a function of the reciprocal of the absolute temperature (T^{-1}) is recorded in Figure 6. That the curves obtained in the form of lines, obey the Arrhenius law, therefore satisfies the relation (4).

Figure 7 shows the variation of $\ln(W_{corr}/T)$ function ($1/T$) as a straight line with a slope of $(-\Delta H_a/R)$ and the intersection with the y-axis is $[\ln(R/Nh) + (\Delta S_a/R)]$. From these relationships, values of ΔS_a and ΔH_a can be calculated. The activation parameters (E_a , ΔH_a and ΔS_a) calculated from the slopes of Arrhenius lines in the absence and presence of our inhibitors (Fig.6 and Fig.7) are summarized in Table 3.

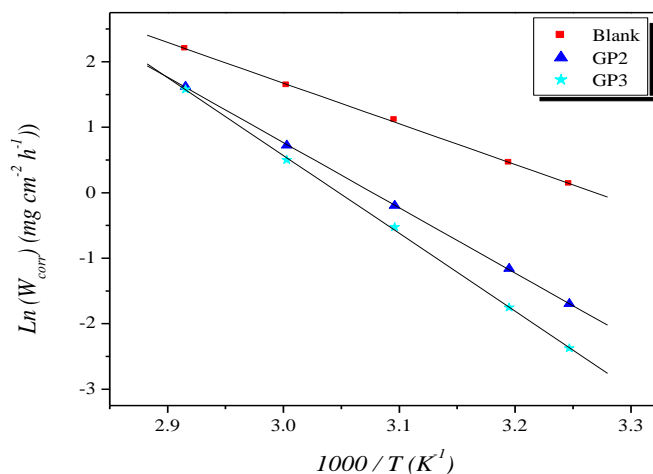


Figure 6. Arrhenius plots of $\ln W_{corr}$ vs. $1/T$ for steel in 1.0 M HCl in the absence and the presence of GP2 and GP3 at optimum concentration.

According to the report in literature [44], higher value of E_a was considered as physisorption that occurred in the first stage. Because the electrochemical corrosion is relevant to heterogeneous

reactions, the preexponential factor A in the Arrhenius equation is related to the number of active centers. There are two possibilities about these active centers with different E_a on the metal surface: (1) the activation energy in the presence of inhibitors is lower than that of pure acidic medium, $E_a(\text{inh}) < E_a(\text{HCl})$, which suggests a smaller number of more active sites remain uncovered in the corrosion process; (2) the activation energy in the presence of inhibitor is higher than that of pure acidic medium, $E_a(\text{inh}) > E_a(\text{HCl})$, which represents the inhibitor adsorbed on most active adsorption sites (having the lowest energy) and the corrosion takes place chiefly on the active sites (having higher energy).

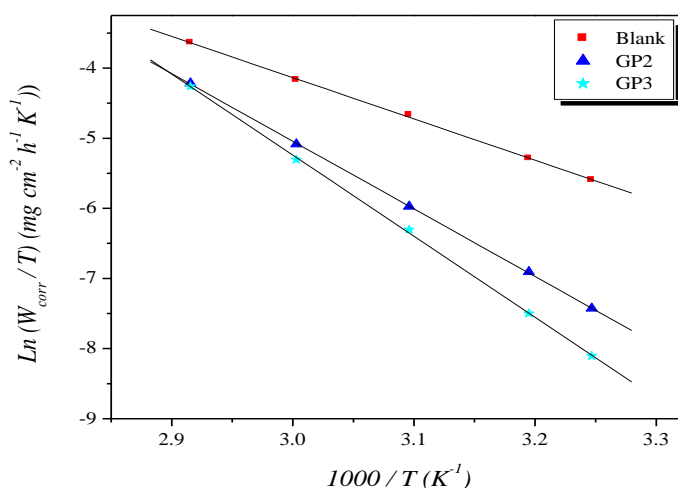


Figure 7. Arrhenius plots of $\text{Ln}(W_{\text{corr}}/T)$ vs. $1/T$ for steel in 1.0 M HCl in the absence and the presence of GP2 and GP3 at optimum concentration.

In this study the values of E_a obtained from the slopes of these straight lines are recorded in Table 3. The values of E_a were higher for inhibited solutions indicating physical adsorption of the inhibitor on the metal surface [45, 46]. However, this energy increases with the addition of the pyridazine compounds into molar solution of hydrochloric acid, which shows a change in the mechanism of transition metal in solution. However, several authors [47-52] showed that the increase in E_a may often be interpreted by the formation of an adsorption film by a physical mechanism (electrostatic).

The values of E_a and ΔH_a was increased in the presence of inhibitors, suggesting that the energy barrier of the corrosion reaction increases, meaning that the dissolution of the steel is difficult [50]. According Gomma et al [51], the activation energy is much higher than the inhibitor is more effective. However, the positive sign of the endothermic enthalpy reflects the nature of the dissolution of the steel. We note that the variation of the activation energy E_a and the enthalpy of ΔH_a vary in the same way with the concentration of inhibitor, which satisfies the relationship between E_a and thermodynamics as ΔH_a [53]: $E_a - \Delta H_a = RT$.

The values of ΔS_a were lower for the solution without inhibitor than that for the solution with inhibitor. This might be attributed to the rate-determining step for the activated complex was the

association rather than the dissociation step [54]. As seen from Table 3, the shift of ΔS_a to more positive values in the presence of the inhibitor, thus the increase in disorder is a driving force that can overcome the barriers for the adsorption of inhibitor onto the metal surface.

Table 3. Activation parameters for the steel dissolution in 1.0 M HCl in the absence and the presence of GP2 and GP3 at 10^{-3} M.

Inhibitors	A ($\text{mg}/\text{cm}^2 \text{ h}$)	Linear regression coefficient (r)	E_a (kJ/mol)	ΔH_a (kJ/mol)	ΔS_a (J/mol.K)	$E_a - \Delta H_a$ (kJ/mol)
Blank	$6,6808 \times 10^8$	0.99976	51.67	48.97	-85.00	2.7
GP2	2.0500×10^{13}	0.99996	82.83	80.13	0.910	2.7
GP3	5.2800×10^{15}	0.99984	98.76	96.06	47.06	2.7

3.1.3. Adsorption isotherm and thermodynamic parameters

The inhibition of corrosion of metals by organic compounds is explained by their adsorption. The latter is described by two main types of adsorption, namely physical adsorption and chemical adsorption. It depends on the charge of the metal, the nature of the chemical structure of the organic product and the type of electrolyte. The presence of a transition metal, having orbital "d" vacant, and a molecule having centers that facilitates electron rich adsorption [55,56].

The organic inhibitors are compounds having at least one active center of the chemisorption (hetero multiple bonds or aromatic rings having π electrons). In the case of aromatic compounds, the electron density will be affected by the introduction of substituent's, which increases or decreases the corrosion-inhibiting effectiveness.

The adsorption isotherm can be determined if the mode of action of the inhibitor is mainly due to adsorption on the metal surface. And the type of these isotherms can provide additional information regarding the inhibitory properties of the compounds tested. However, if we assume that the adsorption of our inhibitors adsorption isotherm follows Langmuir, the rate of surface coverage (θ) for different concentrations in acidic medium is evaluated by the method of weight loss according to the report E_w (%) / 100 and using the following equation [57]:

$$\frac{C_{\text{inh}}}{\theta} = \frac{1}{K_{\text{ads}}} + C_{\text{inh}} \quad (6)$$

Where K_{ads} denotes the equilibrium constant for the adsorption process.

Figure 8 shows the curves of the variation of C_{inh} / θ according to the concentration C_{inh} for the pyridazine compounds. The linearity of these curves indicates that the adsorption of our inhibitors on the surface of C38 steel in 1.0 M HCl, is according to the Langmuir isotherm model checking equation (6). The validity of this approach is confirmed by the strong correlation ($R^2 = 0.99992$ for the compound GP2 and $R^2 = 0.99988$ for GP3).

The values of K_{ads} obtained from the reciprocal of intercept of Langmuir isotherm line are listed in Table 4, together with the values of the Gibbs free energy of adsorption ΔG_{ads}° calculated from the equation:

$$\Delta G_{ads}^\circ = -RTL \ln(55.5 K_{ads}) \tag{7}$$

where R is the universal gas constant, T the thermodynamic temperature and the value of 55.5 is the concentration of water in the solution [58].

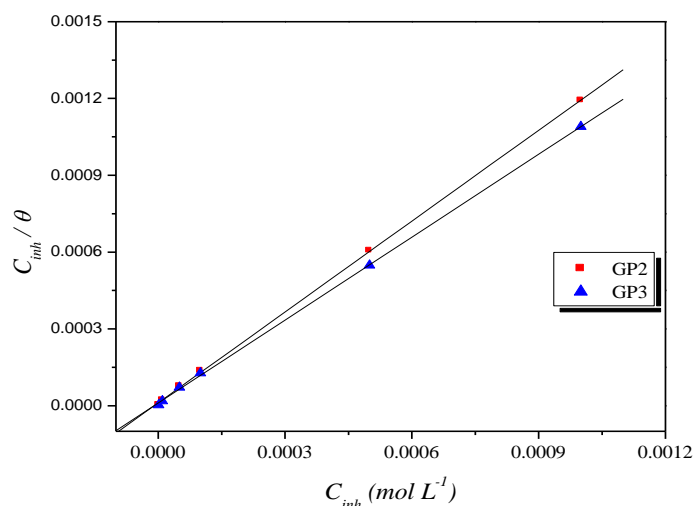


Figure 8. Langmuir adsorption of GP2 and GP3 on the steel surface in 1.0 M HCl solution.

Table 4. Thermodynamic parameters for the adsorption of GP2 and GP3 in 1.0 M HCl on the C38 steel at 308K

Inhibitors	Slopes	$K_{ads} (M^{-1})$	R^2	$\Delta G_{ads}^\circ (kJ/mol)$
GP2	1.18	90331.79	0.99992	-39.53
GP3	1.08	94209.86	0.99988	-39.63

The high values of adsorption equilibrium constants K_{ads} correspondent's pyridazines GP3 and GP2 to reflect the high adsorption capacity of these inhibitors on the surface of C38 steel in acidic 1.0 M HCl. This suggests that these inhibitors can best recoveries, where their most effective protection against corrosion. However, the value of K_{ads} of GP3 is superior to that of GP2, which in agreement with the effective inhibitory GP3 compared to GP2.

The negative values of the standard free energy of adsorption indicates a spontaneous adsorption of molecules on the surface of our C38 steel and also the strong interaction between the inhibitors molecules and the metal surface [59,60]. In general, the standard values of free energy of -20 kJ mol^{-1} or less negative are associated with an electrostatic interaction between the charged molecules and charged metal surface (physical adsorption), those from -40 kJ mol^{-1} or more negative involves a

load sharing or transfer inhibitor molecules to the metal surface to form a coordinate covalent bond (chemisorption) [61-63]. The values of ΔG_{ads}° in our measurements (in Table 4) is $-39.63 \text{ kJ mol}^{-1}$ for GP3 and $-39.53 \text{ kJ mol}^{-1}$ for GP2, it is suggested that the adsorption of this GP3 and GP2 involves two types of interactions: chemisorption and physisorption [64].

The values of the heat of adsorption were evaluated from the kinetic thermodynamic model [65, 66]:

$$\left[\frac{\theta}{1-\theta} \right] = AC \exp\left(\frac{-Q_{ads}}{RT}\right) \tag{8}$$

where A is a constant, C is the inhibitor concentration, θ is the occupied, $(1 - \theta)$ is the vacant site not occupied by the inhibitor and Q_{ads} is heat of adsorption and equal to enthalpy of adsorption (ΔH_{ads}°) process [67]. Figure 9 depicts the plot of $\text{Ln} [\theta/(1 - \theta)]$ as a function of $1/T$ for GP2 and GP3 at optimum concentration. The heats of adsorption (Q_{ads}) are calculated from the slopes of curves as $-46.77 \text{ kJ mol}^{-1}$ and $-63.21 \text{ kJ mol}^{-1}$ for GP2 and GP3, respectively. The negative values of Q_{ads} indicated that the adsorption of used inhibitors on the carbon steel surface is exothermic.

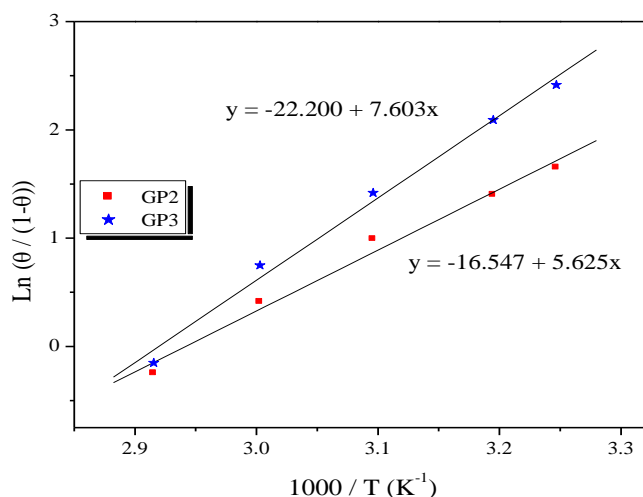


Figure 9. $\text{Ln} (\theta / (1 - \theta))$ vs. $1/T$ for adsorption of GP2 and GP3.

The entropy of adsorption process (ΔS_{ads}°) was obtained based on following thermodynamic basic equation [68, 69]:

$$\Delta G_{ads}^\circ = \Delta H_{ads}^\circ - T\Delta S_{ads}^\circ \tag{9}$$

The values of ΔS_{ads}° was calculated as $-23.51 \text{ J mol}^{-1} \text{ K}^{-1}$ and $-76.56 \text{ J mol}^{-1} \text{ K}^{-1}$ for GP2 and GP3 respectively, The negative values of ΔS_{ads}° might be explained as: before the adsorption of inhibitor onto the steel surface, inhibitor molecules might freely move in the bulk solution (the inhibitor

molecules were chaotic), but with the progress in the adsorption, inhibitor molecules were orderly adsorbed onto the steel surface, as a result, a decrease in entropy [70]. Therefore negative values of ΔS_{ads}° in the present investigation support the higher adsorbability of organic compounds on the metal surface.

3.2. Electrochemical polarisation studies

Polarization measurements have been carried out in order to gain knowledge concerning the kinetics of the anodic and cathodic reactions. Typical potentiodynamic polarization curves of the C38 steel in 1.0 M HCl solutions without and with addition of different concentrations of pyridazine derivatives are shown in Figs. 10-11. Electrochemical kinetic parameters (corrosion potential (E_{corr}), corrosion current density (I_{corr}) and cathodic Tafel slope (β_c)), determined from these experiments by extrapolation method [71], are reported in Table 5. The I_{corr} was determined by Tafel extrapolation of only the cathodic polarization curve alone, which usually produces a longer and better defined Tafel region [72]. The I_{corr} values were used to calculate the inhibition efficiency, $\eta_{Tafel}(\%)$, (listed in Table 5), using the following equation [73]:

$$\eta_{Tafel}(\%) = \frac{I_{corr} - I_{corr(i)}}{I_{corr}} \times 100 \quad (10)$$

where I_{corr} and $I_{corr(i)}$ are the corrosion current densities for steel electrode in the uninhibited and inhibited solutions, respectively.

Table 5. Polarization data of C38 steel in 1.0 M HCl without and with addition of inhibitors at 308 K.

Inhibitor	Conc (M)	$-E_{corr}$ (mV/SCE)	$-\beta_c$ (mV dec ⁻¹)	I_{corr} ($\mu\text{A cm}^{-2}$)	η_{Tafel} (%)
HCl	1.0	455.2	127.3	815.7	-----
	10^{-3}	472.3	121.7	130.9	83.9
GP2	10^{-4}	464.4	112.3	221.1	72.9
	10^{-5}	466.3	118.4	430.5	47.2
	10^{-6}	445.0	118.9	494.5	39.5
	10^{-3}	470.2	132.3	091.9	88.7
GP3	10^{-4}	479.4	105.4	202.0	75.2
	10^{-5}	460.6	118.1	371.9	54.4
	10^{-6}	473.0	112.9	484.0	40.7

The results in Table 5 show that the inhibition efficiency increased, while the corrosion current density decreased with the addition of inhibitors. This may be due to the adsorption of inhibitors on C38 steel/acid interface. The lowest I_{corr} value ($91.9 \mu\text{A cm}^{-2}$) and best inhibition efficiency was

obtained for GP3 at 10^{-3} M. The results in Table 5 indicated that the increase of inhibition efficiency with concentration might be attributed to the formation of the barrier film which prevented acid medium from attacking the metal surface.

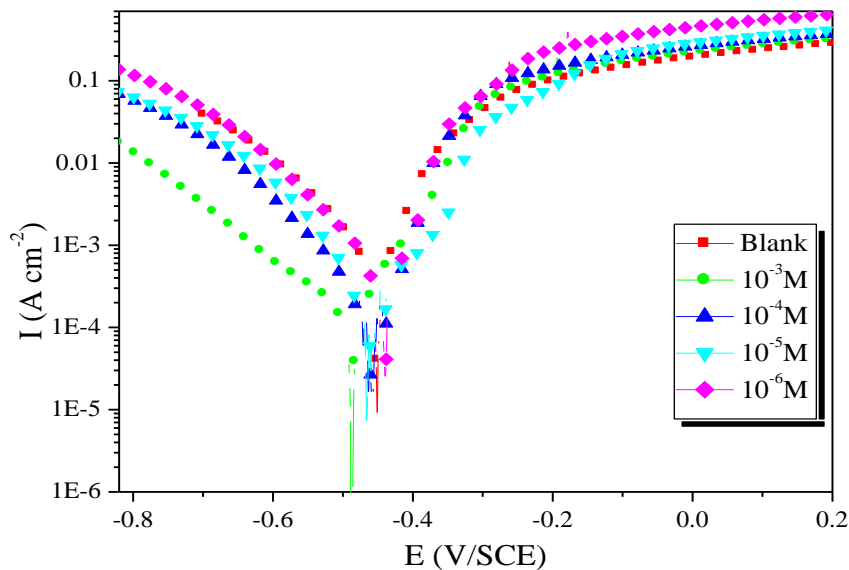


Figure 10. Polarization curves of C38 steel in 1.0 M HCl containing different concentrations of GP2.

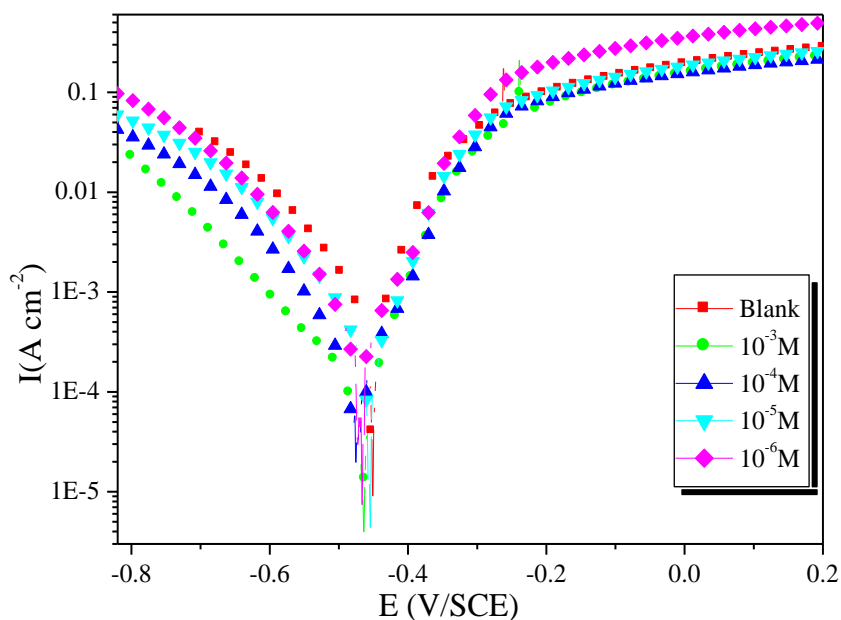


Figure 11. Polarization curves of C38 steel in 1.0 M HCl containing different concentrations of GP3.

E_{corr} values was shifted towards less negative potential which is a necessary to quote the inhibitive action of inhibitor and to classify an inhibitor into an anodic, a cathodic, or mixed type. It has been reported that [74], an inhibitor can be classified as an anodic or a cathodic-type inhibitor on

the basis of magnitude of shift in E_{corr} value. If displacement in E_{corr} is greater than 85 mV, towards anode or cathode with reference to blank, then an inhibitor is categorized as either anodic or cathodic type inhibitor, respectively. Otherwise an inhibitor is treated as mixed type. In our study, maximum displacement in E_{corr} value was around 24.2 mV indicating pyridazine derivatives area mixed type inhibitor, in 1.0 M HCl. Figs. 10-11 represents the polarisation curves of C38 steel in 1.0 M HCl without and with the different inhibitors in concentrations of 10^{-3} - 10^{-6} M by weight at 308 K. It is clear from Figs. 10-11 that the cathodic current densities decrease with increasing the concentrations of the inhibitors; this indicates that these compounds are adsorbed on the metal surface and hence inhibition occurs. Thus, the addition of these inhibitors hindered the acid attack on the C38 steel electrode. The parallel cathodic Tafel curves in Figs. 10-11 reveal that the hydrogen evolution is activation-controlled and the hydrogen evolution reaction (reduction mechanism) is not affected by the presence of the inhibitors [75].

According to the method of polarization GP3 The compound is considered to be the best inhibitor compared to GP2, which is the maximum inhibition efficiency, reaching 88.73% at a concentration of 10^{-3} M. This is in good agreement with measurements made by the method of weight loss. GP3 > GP2

3.2. Electrochemical impedance spectroscopy

The effect of inhibitor concentration on the impedance behavior of C38 carbon steel in 1.0 M HCl solution at 308 K is presented in Figs. 12-13. The curves show a similar type of Nyquist plot for C38 steel in the presence of various concentrations of GP2 and GP3. In Figs. 12-13, the Nyquist plots contain a very small depressed semicircle, with the center below the real X-axis, whose size is increased by increasing the inhibitor concentration, indicating that the corrosion is mainly a charge transfer process [76]. A loop is also seen at low frequencies which could arise from the adsorbed intermediate products such as $(\text{FeCl})_{\text{ads}}$ in the absence of inhibitor and/or $(\text{FeClInh}^+)_{\text{ads}}$ in the presence of inhibitor according to the mechanism proposed by Solmaz et al [77] for the corrosion of C38 steel in 1.0 M HCl solution. The depressed semicircle is characteristic of solid electrodes and often refers to frequency dispersion which arises due to the substrate roughness and inhomogeneities of the surface [78]. It is clear that the impedance response of C38 steel is significantly changed after addition of inhibitors (P2 and GP3).

Data in Table 5 shows that additional GP2 and GP3 inhibits the corrosion of C38 steel in 1.0 M HCl. The inhibition efficiency increased by increasing the concentration of the studied inhibitors. The inhibition efficiency is calculated using charge transfer resistance from equation [78]:

$$\eta_z(\%) = \frac{R_{ct(\text{inh})} - R_{ct}}{R_{ct(\text{inh})}} \times 100 \quad (11)$$

where R_{ct} and $R_{ct(\text{inh})}$ are the charge transfer resistance values in absence and presence of inhibitor for C38 steel in 1.0 M HCl, respectively.

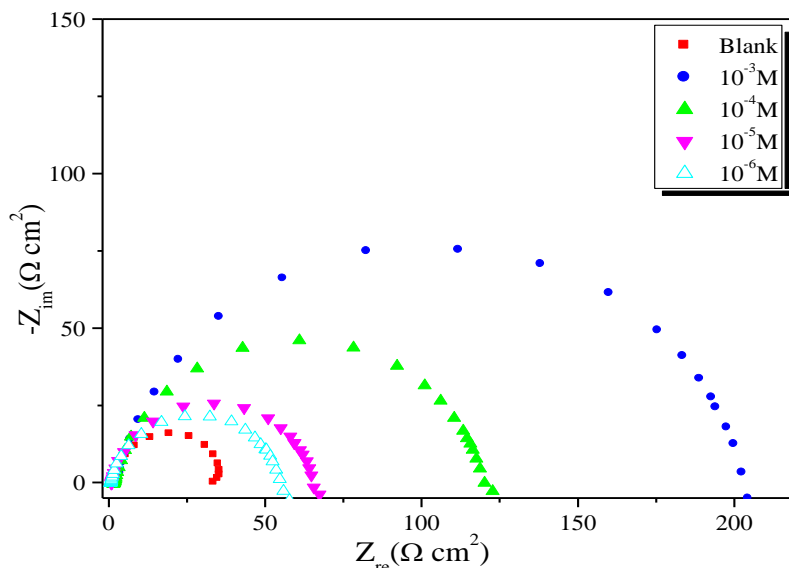


Figure 12. Nyquist diagrams C38 steel in 1.0 M HCl without and with different concentrations of GP2 inhibitor.

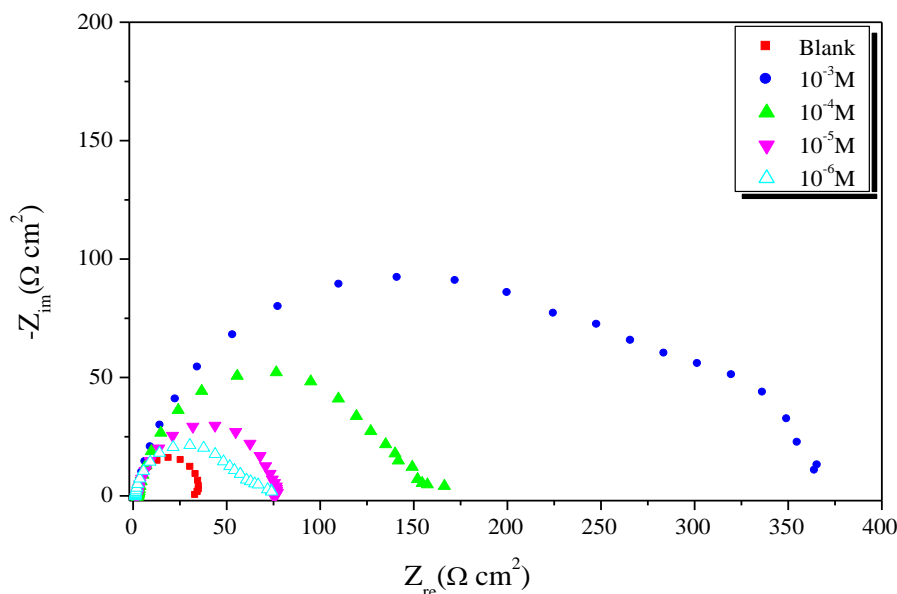


Figure 13. Nyquist diagrams C38 steel in 1.0 M HCl without and with different concentrations of GP3 inhibitor.

For analysis of the impedance spectra containing a single capacitive semicircle, the standard Randle’s circuit is used [79] (Fig. 14), where the circuit is composed of a solution resistance component (R_s) and a capacitance component (C_{dl}). The resistor R_s is in series to the double layer capacitance and R_{ct} while double layer capacitance is parallel to R_{ct} . Similar figures have been described in literature for the acidic corrosion of iron and carbon steel in the presence and absence of

various inhibitor molecules [80,81]. Double layer capacitance values (C_{dl}) were obtained at maximum frequency (f_{max}), at which the imaginary component of the Nyquist plot is maximum and calculated using Eq. (12) [82]:

$$C_{dl} = \frac{1}{2\pi f_{max} R_{ct}} \tag{12}$$

At higher frequencies, the intercept corresponds to the solution resistance (R_s), and at lower frequency end corresponds to ($R_s + R_{ct}$). The difference between these two values gives the charge transfer resistance (R_{ct}). The value of R_{ct} is a measure of the electron transfer across the surface and is inversely proportional to corrosion rate [80]. The impedance parameters like R_{ct} , R_s , C_{dl} values and percentage inhibition efficiency (η_z %) calculated from the R_{ct} values are given in the Table 5. The results also show that R_{ct} values increased with increase in additive concentration. The percentage inhibition efficiencies calculated from the R_{ct} values indicate that pyridazine derivatives acts as a good corrosion inhibitors for corrosion reaction of C38 steel in 1.0 M HCl solution. The C_{dl} values found to decrease with increase the inhibitor concentration in the solutions. This behaviour is generally seen for system where inhibition occurred due to the formation of a surface film by the adsorption of inhibitor on the metal surface [83-85].

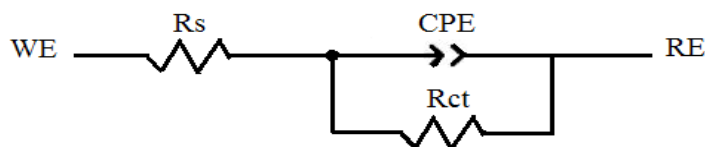


Figure 14. Equivalent circuit for the corrosion behaviour of studied systems.

Table 5. Impedance parameters for corrosion of steel in 1.0 M HCl in the absence and presence of different concentrations of pyridazine derivatives at 308 K.

Inhibitors	Conc (M)	R_s ($\Omega\text{ cm}^2$)	R_{ct} ($\Omega\text{ cm}^2$)	f_{max} (Hz)	C_{dl} ($\mu\text{F cm}^{-2}$)	η_z (%)
HCl	1.0	2.03	033.2	50.00	095.8	-----
GP2	10^{-3}	0.96	203.7	28.09	027.8	83.7
	10^{-4}	1.08	118.7	28.09	047.8	72.0
	10^{-5}	1.36	064.7	25.00	098.4	48.7
	10^{-6}	1.87	055.3	25.00	115.2	39.9
GP3	10^{-3}	0.84	273.2	25.00	023.3	87.8
	10^{-4}	1.04	133.6	31.65	037.7	75.1
	10^{-5}	1.22	073.9	28.09	076.7	55.1
	10^{-6}	1.58	055.7	35.71	080.0	40.4

Decrease in C_{dl} , which can result from a decrease in local dielectric constant and/or an increase in the thickness of the electrical double layer, suggests that the inhibitor molecules act by adsorption at

the metal/solution interface [86]. The sequence of the inhibitors efficiencies were following the order of GP3 > GP2 which is in agreement with the results obtained from the polarization technique.

Fig.15 which represents the variation of the charge transfer resistance of the double layer capacitance and the inhibition efficiency of two pyridazine studied, shows that with the increase in concentration there will be a decrease in the C_{dl} value and an increase in the values of R_{ct} and E (%).

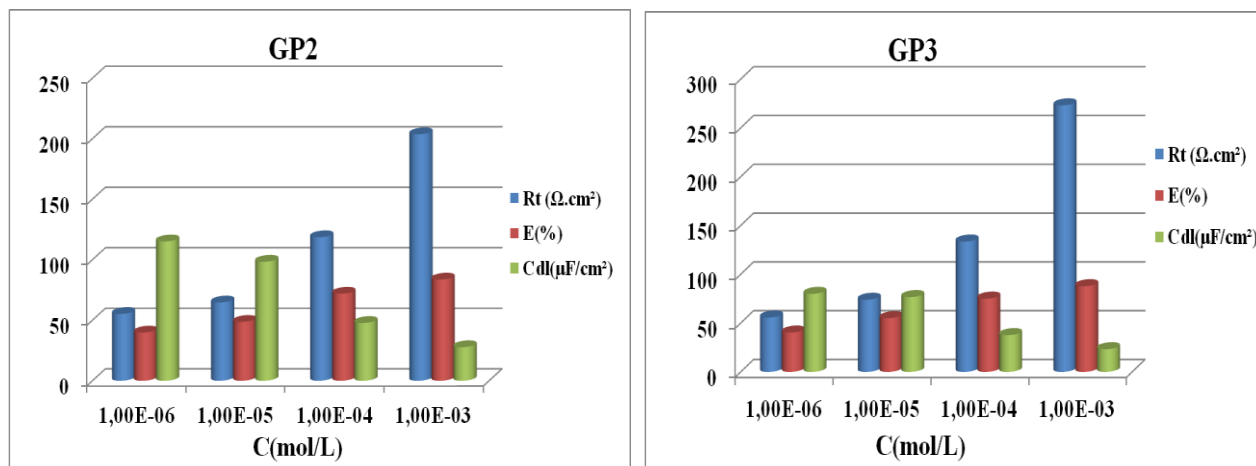


Figure 15. Evolution of the charge transfer resistance, the efficiency of inhibition and the double layer capacitance as a function of the concentration of GP2 and GP3.

A comparative study can be made between the efficiencies inhibitions E (%) obtained by the three known methods (weight loss, polarization curves and EIS methods) by plotting the graph of the variation of E (%) depending on the concentration (Fig. 16). We can deduce that, whatever the method used, no significant change was observed in the E (%) values. We can therefore conclude that there is a good correlation with the three methods used in this investigation at all concentrations tested and our pyridazines are effective inhibitors of corrosion of C38 steel.

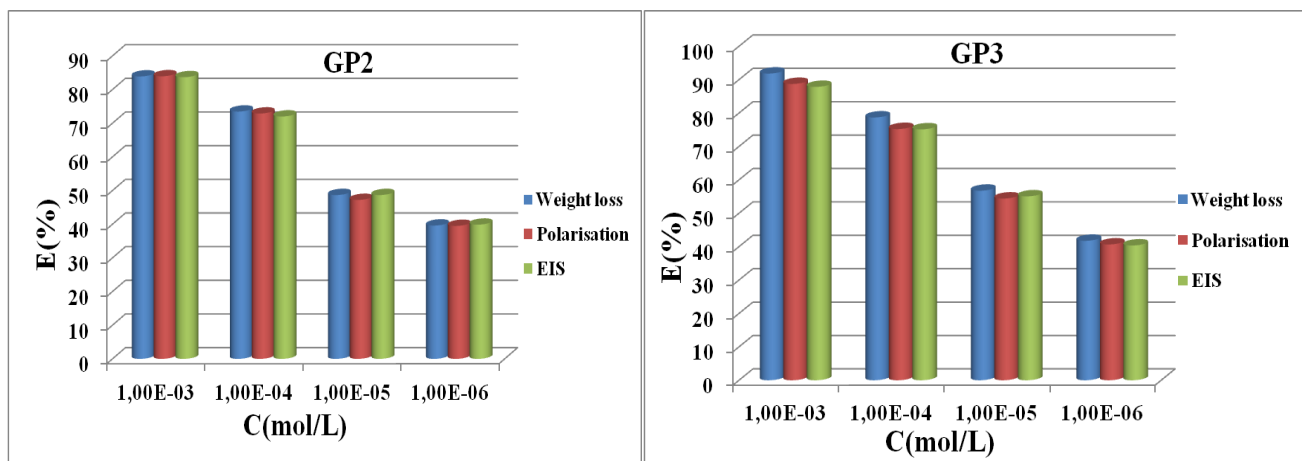


Figure 16. Comparison of inhibition efficiency (E %) values obtained by weight loss, polarization and EIS methods.

4. CONCLUSION

The corrosion behaviour of C38 steel was investigated in 1.0 M HCl with and without addition of various concentrations of two pyridazine derivatives at concentrations using gravimetric, polarisation and electrochemical impedance techniques. Polarisation curves reveal that these compounds are acted as mixed type (cathodic/anodic) inhibitors and inhibition efficiency (%) increases with increasing concentration of inhibitors. Impedance method indicates that compounds adsorbs on C38 steel surface with increasing charge transfer resistance and decreasing the double-layer capacitance. The adsorption of these compounds on C38 steel in 1.0 M HCl solution obeys Langmuir adsorption isotherm. The negative values of ΔG_{ads}° show the spontaneity of the adsorption.

ACKNOWLEDGEMENTS

Prof S. S. Al-Deyab and Prof B. Hammouti extend their appreciation to the Deanship of Scientific Research at king Saud University for funding the work through the research group project.

References

1. A.F. Gualdrón, E.N. Becerra, D.Y. Peña, J.C. Gutiérrez, H.Q. Becerra, *J. Mater. Environ. Sci.* 4 (2013) 143.
2. H. Zarrok, R. Salghi, A. Zarrouk, B. Hammouti, H. Oudda, Lh. Bazzi, L. Bammou, S. S. Al-Deyab, *Der Pharm. Chem.* 4 (2012) 407.
3. H. Zarrok, S. S. Al-Deyab, A. Zarrouk, R. Salghi, B. Hammouti, H. Oudda, M. Bouachrine, F. Bentiss, *Int. J. Electrochem. Sci.* 7 (2012) 4047.
4. D. Ben Hmamou, R. Salghi, A. Zarrouk, H. Zarrok, B. Hammouti, S. S. Al-Deyab, M. Bouachrine, A. Chakir, M. Zougagh, *Int. J. Electrochem. Sci.* 7 (2012) 5716.
5. A. Zarrouk, B. Hammouti, S.S. Al-Deyab, R. Salghi, H. Zarrok, C. Jama, F. Bentiss, *Int. J. Electrochem. Sci.* 7 (2012) 5997.
6. A. Zarrouk, H. Zarrok, R. Salghi, B. Hammouti, S.S. Al-Deyab, R. Touzani, M. Bouachrine, I. Warad, T. B. Hadda, *Int. J. Electrochem. Sci.* 7 (2012) 6353.
7. A. Zarrouk, M. Messali, H. Zarrok, R. Salghi, A. Al-Sheikh Ali, B. Hammouti, S. S. Al-Deyab, F. Bentiss, *Int. J. Electrochem. Sci.* 7 (2012) 6998.
8. H. Zarrok, A. Zarrouk, R. Salghi, Y. Ramli, B. Hammouti, S. S. Al-Deyab, E. M. Essassi, H. Oudda, *Int. J. Electrochem. Sci.* 7 (2012) 8958.
9. D. Ben Hmamou, R. Salghi, A. Zarrouk, H. Zarrok, S. S. Al-Deyab, O. Benali, B. Hammouti, *Int. J. Electrochem. Sci.* 7 (2012) 8988.
10. A. Zarrouk, M. Messali, M. R. Aouad, M. Assouag, H. Zarrok, R. Salghi, B. Hammouti, A. Chetouani, *J. Chem. Pharm. Res.* 4 (2012) 3427.
11. D. Ben Hmamou, M. R. Aouad, R. Salghi, A. Zarrouk, M. Assouag, O. Benali, M. Messali, H. Zarrok, B. Hammouti, *J. Chem. Pharm. Res.* 4 (2012) 3489.
12. H. Zarrok, H. Oudda, A. El Midaoui, A. Zarrouk, B. Hammouti, M. Ebn Touhami, A. Attayibat, S. Radi, R. Touzani, *Res. Chem. Intermed* (2012) DOI 10.1007/s11164-012-0525-x
13. A. Zarrouk, A. Dafali, B. Hammouti, H. Zarrok, S. Boukhris, M. Zertoubi, *Int. J. Electrochem. Sci.* 5 (2010) 46.
14. A. Zarrouk, T. Chelfi, A. Dafali, B. Hammouti, S.S. Al-Deyab, I. Warad, N. Benchat, M. Zertoubi, *Int. J. Electrochem. Sci.* 5 (2010) 696.

15. A. Zarrouk, I. Warad, B. Hammouti, A. Dafali, S.S. Al-Deyab, N. Benchat, *Int. J. Electrochem. Sci.* 5 (2010) 1516.
16. A. Zarrouk, B. Hammouti, R. Touzani, S.S. Al-Deyab, M. Zertoubi, A. Dafali, S. Elkadiri, *Int. J. Electrochem. Sci.* 6 (2011) 4939.
17. A. Zarrouk, B. Hammouti, H. Zarrok, S.S. Al-Deyab, M. Messali, *Int. J. Electrochem. Sci.* 6 (2011) 6261.
18. A. Chetouani, B. Hammouti, A. Aouniti, N. Benchat and T. Benhadda, *Prog. Org. Coat.* 45 (2002) 373.
19. A. Chetouani, B. Hammouti, A. Aouniti, N. Benchat, T. Benhadda, *Prog. Org. Coat.* 45 (2003) 73.
20. A. Chetouani, A. Aouniti, B. Hammouti, N. Benchat, T. Benhadda, S. Kertit, *Corros. Sci.* 45 (2003) 1675.
21. M. Bouklah, N. Benchat, B. Hammouti, A. Aouniti, S. Kertit, *Mater. Lett.* 60 (2006) 1901.
22. N.A. Negm, A.M. Al Sabagh, M.A. Migahed, H.M. Abdel Bary, H.M. El Din, *Corros. Sci.* 52 (2010) 2122.
23. H. Zarrok, H. Oudda, A. Zarrouk, R. Salghi, B. Hammouti, M. Bouachrine; *Der Pharm. Chem.* 3 (2011) 576.
24. F. Bentiss, M. Outirite, M. Traisnel, H. Vezin, M. Lagrenée, B. Hammouti, S.S. Al-Deyab, C. Jama, *Int. J. Electrochem. Sci.* 7 (2012) 1699.
25. A. Zarrouk, B. Hammouti, H. Zarrok, R. Salghi, A. Dafali, Lh. Bazzi, L. Bammou, S. S. Al-Deyab, *Der Pharm. Chem.* 4 (2012) 337.
26. B. Zerga, R. Saddik, B. Hammouti, M. Taleb, M. Sfaira, M. Ebn Touhami, S.S. Al-Deyab, N. Benchat, *Int. J. Electrochem. Sci.* 7 (2012) 631.
27. B. Abdelnabi, N. Khalil, A. Mohamed, *Surf. Technol.* 24 (1985) 383.
28. M. Bouklah, N. Benchat, A. Aouniti, B. Hammouti, M. Benkaddour, M. Lagrenée, H. Vezin, F. Bentiss, *Prog. Org. Coat.* 51 (2004) 118.
29. M.A. Quraishi, J. Rawat, *Mater. Chem. Phys.* 77 (2002) 43.
30. O. Benali, H. Benmehdi, O. Hasnaoui, C. Selles, R. Salghi, *J. Mater. Environ. Sci.* 4 (2013) 127.
31. A. Popova, M. Christov, S. Raicheva, E. Sokolova, *Corros. Sci.* 46 (2004) 1333.
32. L.M. Vracar, D.M. Drazic, *Corros. Sci.* 44 (2002) 1669.
33. M. Bouklah, B. Hammouti, A. Aouniti, T. Benhadda, *Prog. Org. Coat.* 47 (2004) 225.
34. D. Bouzidi, S. Kertit, B. Hammouti, M. Brighli, *J. Electrochem. Soc. India.* 46 (1997) 23.
35. M. Abdulwahab, A. Kasim, O. S. I. Fayomi, F. Asuke, A. P. I. Popoola, *J. Mater. Environ. Sci.* 3 (2012) 1177.
36. E. McCafferty, *Corrosion Control by Coating*, H. Leidheiser Editor, Science Press, Princeton, N.J. (1979) 279.
37. A. Dafali, B. Hammouti, S. Kertit, *J. Electrochem. Soc. India.* 50 (2001) 62.
38. J.G.N. Thomas, in: *5th Eur. Symp. On Corros. Inhibitors*, Ann. Univ. Ferrara, Italy. (1980-1981) 453.
39. P. Coudert, C. Rubat, E. Duroux, P. Bastide, J. Couquelet, P. Tronche, E. Albuissou, *Farmaco.* 47 (1992) 37.
40. S. Moreau, P. Coudert, B. Lasserre, D. Vallee-Goyet, D. Gardette, C. Navarro-Delmas, A.P. Huu Chanh, V. Dossou-Gbete, J. Couquelet, *Prostaglandins Leukot. Essent. Fat. Acids* 56 (1997) 431.
41. B. Bonnelly, T.C. Downie, R. Grzekowiak, H.R. Hamburg, D. Short, *Corros. Sci.* (1978) 18.
42. H. Brandt, M. Fischer, K. Schawabe, *Corros. Sci.* 10 (1970) 631.
43. J. O'M. Bockris, A. K. N. Reddy, *Modern. Electrochem. Plenum Press, New York.* 2 (1977) 1267.
44. W. Chen, H.Q. Luo, N.B. Li, *Corros. Sci.* 53 (2011) 335.
45. H. Zarrok, K. Al Mamari, A. Zarrouk, R. Salghi, B. Hammouti, S. S. Al-Deyab, E. M. Essassi, F. Bentiss, H. Oudda, *Int. J. Electrochem. Sci.*, 7 (2012) 10338.
46. F. Bentiss, M. Lebrini, M. Lagrenée, *Corros. Sci.* 47 (2005) 2915.

47. E.E. Foad El Sherbini, *Mat. Chem. Phys.* 60 (1999) 286.
48. K.F. Khaled, A. El-mghraby, O.B. Ibrahim, O.AEIhabib, A.M. Magdy Ibrahim, *J. Mater. Environ. Sci.* 1 (2010) 139.
49. N.P. Clark, E. Jakson, M. Robinson, *Br. Corros. J.* 14 (1979) 33.
50. T. Szauer, A. Brand, *Electrochim. Acta.* 26 (1981) 1219.
51. G.K. Gomma, M.H. Wahdan, *Mater. Chem. Phys.* 39 (1995) 209.
52. N.M. Guan, L. Xueming and L. Fei, *Mater. Chem. Phys.* 86 (2004) 59.
53. M. Stern, A. L. Geary, *J. Electrochem. Soc.* 104 (1957) 56.
54. A.K. Singhn M.A. Quraishi, *J. Mater. Environ. Sci.* 1 (2010) 101.
55. A.H. Mehaute, G. Grepy, *Solid State Ionics.* 9 (1989) 17.
56. K.B. Samardzija, C. Lupu, N. Hackerman, A.R. Barron, *J. Mater. Chem.* 15 (2005) 1908.
57. I. Langmuir, *J. Am. Chem. Soc.* 39 (1917) 1848.
58. J. Flis, T. Zakroczymski, *J. Electrochem. Soc.* 143 (1996) 2458.
59. I. El Ouali, B. Hammouti, A. Aouniti, Y. Ramli, M. Azougagh, E.M. Essassi, M. Bouachrine, *J. Mater. Environ. Sci.* 1 (2010) 1.
60. G. Avci, *Mater. Chem. Phys.* 112 (2008) 234.
61. V. Bransoi, M. Baibarac, F. Bransoi, *International. Cong. Chemical Engineering, Romania.* (2001) 215
62. E. Bayol, A.A. Gurten, M. Dursun, K. Kayakırlmaz, *Acta Phys. Chim. Sin.* 24 (2008) 2236.
63. O.K. Abiola, N.C. Oforika, *Mater. Chem. Phys.* 83 (2004) 315.
64. M. Ozcan, R. Solmaz, G. Kardas, I. Dehri, *Colloid Surf. A.* 325 (2008) 57.
65. M.K. Gomma, W.H. Wahdan, *Bull. Chem. Soc. Jpn.*, 67 (1994) 1.
66. E.E. Oguzie, V.O. Njoku, C.K. Enenebeaku, C.O. Akalezi, C. Obi, *Corros. Sci.*, 50 (2008) 3480.
67. C.W. Tang, *Appl. Phys. Lett.*, 48 (1986) 183.
68. G. Avci, *Colloid. Surf. A.* 317 (2008) 730.
69. S.M.A. Hosseini, A. Azimi, *Corros. Sci.* 51 (2009) 728.
70. L. Tang, X. Li, L. Li, Q. Qu, G. Mu, G. Liu, *Mater. Chem. Phys.* 94 (2005) 353.
71. M. Lebrini, F. Bentiss, N. Chihib, C. Jama, J.P. Hornez, M. Lagrenée, *Corros. Sci.* 50 (2008) 2914.
72. E. McCafferty, *Corros. Sci.* 47 (2005) 3202.
73. M. Larif, A. Elmidaoui, A. Zarrouk, H. Zarrok, R. Salghi, B. Hammouti, H. Oudda, F. Bentiss, *Res. Chem. Intermed* (2012) DOI: 10.1007/s11164-012-0788-2.
74. Ishtiaque Ahamad, Rajendra Prasad, M.A. Quraishi, *Corros. Sci.* 52 (2010) 1472.
75. M.A. Hegazy, H.M. Ahmed, A.S. El-Tabie, *Corros. Sci.* 53 (2011) 671.
76. F. Bentiss, M. Lagrenée, M. Traisnel, J.C. Hornez, *Corros. Sci.*, 41 (1999) 789.
77. R. Solmaz, G. Kardas, M. Culha, B. Yazici, M. Erbil, *Electrochim. Acta.*, 53 (2008) 5941.
78. A. Zarrouk, H. Zarrok, R. Salghi, N. Bouroumane, B. Hammouti, S. S. Al-Deyab, R. Touzani, *Int. J. Electrochem. Sci.*, 7 (2012) 10215.
79. G. Achary, H.P. Sachin, Y. Arthoba Naik, T.V. Venkatesha, *Mater. Chem. Phys.* 107 (2008) 44.
80. H. Ashassi-Sorkhabi, B. Shaabani, D. Seifzadeh, *Appl. Surf. Sci.* 239 (2005) 154.
81. M. Bouklah, B. Hammoutin, M. Benkaddoun, T. Benhadda, *J. Appl. Electrochem.* 35 (2005) 1095.
82. F. Mansfeld, M.W. Kending, W.J. Lorenz, *J. Electrochem. Soc.* 132 (1985) 290.
83. M. Behpour, S.M. Ghoreishi, N. Soltani, M.S. Niasari, *Corros. Sci.* 51 (2009) 1073.
84. N.A. Negm, F.M. Ghuiba, S.M. Tawfik, *Corros. Sci.* 53 (2011) 3566.
85. D.P. Schweinsberg, G.A. George, A.K. Nanayakkara, D.A. Steiner, *Corros. Sci.* 28 (1988) 33.
86. G. Bereket, A. Yurt, *Corros. Sci.* 43 (2001) 1179.